Pakistan Veterinary Journal

ISSN: 0253-8318 (PRINT), 2074-7764 (ONLINE)
DOI: 10.29261/pakvetj/2024.129

RESEARCH ARTICLE

Silymarin Reduces Paclitaxel-induced Lung Damage Via Down-regulating P2X7R Expression and Inhibiting Inflammation and Apoptosis in the Rats

Nevra Aydemir Celep[*1,2], Elif Erbaş[1], Hülya Kara[3] and Adem Kara[4]

[1]Atatürk University, Faculty of Veterinary Medicine, Department of Histology and Embryology, Erzurum/Turkey
[2]Atatürk University, Faculty of Medicine, Department of Pharmacology, Erzurum/Turkey
[3]Atatürk University, Faculty of Veterinary, Department of Anatomy, Turkey
[4]Erzurum Technical University, Molecular Biology and Genetics, Erzurum/Turkey
*Corresponding author: nevraaydemir@hotmail.com

ARTICLE HISTORY (23-398)

Received: September 9, 2023
Revised: December 20, 2023
Accepted: January 9, 2024
Published online: January 23, 2024

Key words:
Paclitaxel
Silymarin
Purinergic signaling
Apoptosis
Chemotherapy
Lung toxicity

ABSTRACT

This study explores the impact of silymarin, a potent natural flavonoid with robust antioxidant properties, on paclitaxel-induced lung injury. Paclitaxel, a widely used chemotherapeutic agent for cancer, is known for its adverse effects on various organs. The research involved four groups: the Control group (6 animals) received oral saline; the SIL group (6 animals) received 200 mg/kg silymarin orally for 10 days; the PAX group (6 animals) received intraperitoneal paclitaxel (2 mg/kg) for 5 days; and the PAX+SIL group (6 animals) received both treatments. All groups were sacrificed on the 10th day. Histopathological analysis revealed pathological changes in the lung tissue of the PAX group. Immunopositivity of Bax, iNOS, Nf-kB, and IL-6 antibodies was higher in the PAX group compared to silymarin-treated groups. Conversely, Bcl-2 and MUC1 immunopositivity was lower in the PAX group but higher in silymarin-treated groups. Silymarin administration decreased IL-6, Caspase-3, P2x7 and NF-kB p65 immunoreactivity, while increased Bcl-2 immunoreactivity. Protein expression levels of IL-6, Caspase-3, P2x7, and NF-κB were higher in the PAX group but decreased in the PAX+SIL group. Bcl-2 protein expression was lower in the PAX group but higher in the PAX+SIL group. Additionally, antioxidant enzyme levels increased, while MDA levels decreased in the PAX+SIL group. In conclusion, the findings indicate that silymarin effectively ameliorated paclitaxel-induced lung damage, highlighting its potential therapeutic role in mitigating chemotherapy-related side effects.

To Cite This Article: Celep NA, Erbaş E, Kara A and Kara H, 2024. Silymarin reduces paclitaxel-induced lung damage via down-regulating P2X7R expression and inhibiting inflammation and apoptosis in the rats. Pak Vet J, 44(1): 169-175. http://dx.doi.org/10.29261/pakvetj/2024.129

INTRODUCTION

Nowadays, although there are different methodologies for cancer treatment, radiotherapy and chemotherapy are the most frequently used methods. Taxol is a chemotherapeutic agent produced from the bark of the Taxus brevifolia plant grown in the USA. Taxol is neoadjuvant that was licensed by FDA and is used for ovarian and breast cancer. Its active ingredient is paclitaxel. Paclitaxel increases microtubule accumulation and prevents depolarization in cancer cells that proliferate and spread uncontrollably (Çelik *et al.*, 2020).

Paclitaxel (PAX) and similar drugs produce free radicals and kill cancer cells. However, they might cause secondary tumors in cells without cancer characteristics. Resultant reactive oxygen species may cause damage to cellular DNA, protein, lipid, and carbohydrate molecules. If these damages are not repaired, they might induce cancer. Disruption of the endothelial and epithelial barrier might cause the migration of inflammatory cells to the damaged area. Decreased lung perfusion causes hypoxia (Erbas *et al.*, 2023). According to respiratory function tests performed after neoadjuvant chemotherapy, it was seen that carbon monoxide diffusion capacity decreases. In addition, the incidence of pulmonary complications in postoperative period was also reported to be significantly increased. Paclitaxel is a widely used neoadjuvant chemotherapy drug. Neoadjuvant treatments are thought to damage the lung. Alveolar diffusion is dependent on the normal function of the alveolar-capillary barrier. Besides, tight junctions between endothelial cells and epithelial cells are important components of the alveolar-capillary barrier.

Changes in occludin cause disruption in the integrity of tight junctions between zonula occludens and claudin protein families, and as a result, cellular connections open. Increased permeability in the alveolar-capillary membrane cause deposits of high protein fluids and cells in lung interstitium and alveolar spaces. This leads to pulmonary dysfunction (Le *et al.,* 2012). Furthermore, the use of paclitaxel is shown to affect gas diffusion by damaging the endothelial-epithelial barrier with thickening of the alveolar-capillary membrane and exudation (Liu *et al.,* 2015).

The inflammation role has been attributed to the P2X7 receptors in innate and adaptive immune responses. Considering its crucial role in immune response, it is expected that an imbalance in P2X7 receptor activation may favor several pathological conditions, including inflammatory diseases and cancer. Studies on the pathophysiological functions of purinergic signaling and its therapeutic potential for several disorders have recently been conducted (Burnstock, 2006).

Nowadays, natural antioxidants are widely used to increase cancer-preventing effects and limit the resultant side effects of the drugs used in chemotherapy. One of the antioxidants used for this purpose is silymarin (SIL). Silymarin is an extract of the *Silybum marianum* plant. Silymarin is chemically composed of isosilybin, silybin, silychristine, dehydrosilybin, and silydanin isomers (Taleb *et al.,* 2018). Silymarin a combination of flavonoid and flavonolignan isomers has a broad pharmacological potential including triggering tissue regeneration, removing ROS, facilitating protein, DNA and RNA syntheses, increasing the amount of SOD and preventing peroxidation. Its ability to scavenge free radicals is explained by increasing intracellular GSH density and stabilizing the membrane by preventing lipid peroxidation. In addition, nitric oxide and superoxide anion productions are decreased. In alternative medicine, it could also be used as a hepatoprotective agent (Yardım *et al.,* 2021).

This study was conducted to investigate the potential effects of Silymarin on Paclitaxel-induced lung damage. Various signaling pathways involved in oxidative stress, inflammation and apoptosis were examined using biochemical, histochemical, immunohistochemical, and Western blot techniques.

MATERIALS AND METHODS

Animals housing: Twenty-four male Wistar rats (12-14 weeks old, 270-300 g) were sourced from Medical Experimental Application and Research Center of Atatürk University. Ethical approval (Decision no: 2022/98) guided experimental procedures by the Atatürk University Animal Experiments Local Ethics Committee. Rats were housed in plastic cages under standard lab conditions (23 ± 2°C, 12-hour light/12-hour dark). They had ad libitum access to pellet food and water.

Drugs and treatments: Animals were divided into 4 groups (n=6 each): control group received oral physiological saline via gavage, silymarin (SIL), paclitaxel (PAX) and paclitaxel+silymarin (PAX+SIL). PAX was administered intraperitoneally (i.p.) at a dose of 2 mg/kg for five days (Taksen, Koçak Farma, Türkiye) (Amoateng *et al.,* 2017). Silymarin, in pharmaceutical powdered form, was orally gavaged at 200 mg/kg for 10 days (Cheng *et al.,* 2014).

Sample collection and processing: After the last silymarin administration (24h), animals were euthanized with i.p. sodium pentobarbitone (60 mg/kg) and sacrificed by cervical dislocation. Lung tissues were divided; one part fixed in 10% formaldehyde for 72 hours and the other stored at -80°C for Western blot and oxidative stress analysis.

Biochemical analysis: The lung tissues were homogenized using a 1.15% potassium chloride (KCI) solution to measure tissue malondialdehyde (MDA), glutathione (GSH), glutathione-peroxidase (GPx), and superoxide dismutase (SOD) activities. 1:10 (a/h) homogenate and tissue were isolated as described in a previous study (Çelik *et al.,* 2020). Malondialdehyde (MDA) level was determined colorimetrically as described by previous study (Aydemir Celep *et al.,* 2023). GSH level was determined with the methods proposed by Sedlak and Lindsay (Sedlak and Lindsay, 1968). GSH and MDA levels were given as nmol/g tissue. Absorbance measurements were made with an ELISA plaque reader (Bio-Tek, Winooski, VT, USA). SOD activity was measured according to the method described by Sun *et al*. (Sun *et al.,* 1988). GPx activity was tested in line with procedures developed by Matkovics (Matkovics, 1988). The activity of these enzymes was reported as U/g protein. CAT activity was tested with the Aebi method and the activity was reported as katal/g protein (Aebi, 1983).

Histopathological analysis: Tissues were preserved in 10% formaldehyde for 72 hours to maintain structural integrity and ensure proper fixation of cells and proteins for optimal histological analysis. Subsequently, they were paraffin-embedded through a series of scaled alcohol and xylol steps. 5-µm thick sections from Paraffin blocks were stained with Crossman modified Triple dye and evaluated for histopathology under trinocular light microscopy. Parameters, including pulmonary edema, vascular and alveolar characteristics, and bronchiolar pathology, were graded (0 to 3) based on Passmore *et al.* (2018). Detailed analysis of these characteristics is presented in Table 1, adhering to the referenced protocols.

Immunohistochemical analysis: Lung tissue paraffin blocks (Abcam and Santa Cruz), sectioned at 4 µm, were placed on poly-lysine slides. Sections underwent xylol and alcohol treatment, PBS washing, and 3% H2O2 exposure for endogenous peroxidase inactivation. Antigen retrieval involved 4x5 minutes at 600 watts in citrate solution (pH:6.0). Tissues were treated with protein blocking solution and incubated overnight at +4°C with iNOS (Abcam, ab15323, 1/200 dilution), Bax (Abcam, ab53154, 1/200 dilution), Nf-kB (Santa Cruz, sc-109, 1:200 dilution), Bcl-2 (Santa Cruz, sc-7382, dilution), IL-6 (Abcam, ab208113, 1:100 dilution), and Muc-1 (Santa Cruz, Sc53381, 1:200 dilution) primary antibodies. Secondary antibody (Large Volume Detection System: anti-Polyvalent) and HRP (Thermo Fischer, TP-125-HL)

were applied per manufacturer instructions, with DAB (Thermo Fischer, 3,3′-Diaminobenzidine) as chromogen. After Mayer's Hematoxylin counterstaining, slides were covered with Entellan and examined under a light microscope. Numerical density of immune reactive cells in lung tissue was determined using a stereology workstation (Leica DM4000B; Leica Instruments) and software (Microbrightfield Stereo-Investigator software v. 9.0; Microbrightfield, Williston, VT, USA), as described in Gür *et al.* (2022).

Western blot analysis: Lung tissues were homogenized in RIPA buffer (Ecotech Bio, Turkey) with protease and phosphatase inhibitors using a Qiagen tissue lyser. Total protein was extracted, quantified with a Pierce BCA assay kit (Thermo Sci., USA), and 30 µg protein separated by 10% SDS-PAGE, transferred to a PVDF membrane. After blocking with 5% BSA, membranes were incubated overnight at 4 °C with primary antibodies (P2X7, Caspase-3, Bcl-2, IL-6, Nf-kB, and Beta-actin) at 1:1000 dilution. Following washing, membranes were incubated with HRP-conjugated secondary antibody (Santa Cruz) and protein bands visualized with ECL substrate (Thermo). Analysis used Bio-Rad's Image Lab™ Software.

Statistical analysis: Study data were analyzed using SPSS 20.00. Normal distribution was confirmed (asimp. Sig.), and statistical analysis employed one-way ANOVA. Tukey test compared four independent groups, with $p < 0.05$ considered statistically significant.

RESULTS

Biochemical results: When biochemical oxidative stress parameters were evaluated, tissue MDA levels were found significantly higher in the PAX group ($p<0.05$). In the control, SIL and PAX+SIL groups this value was lower than PAX group and there was not a significant difference. GSH, SOD, GPx and CAT parameters were lower in control, SIL and PAX+SIL groups, and significantly higher in the PAX group ($p<0.05$). Oxidative stress parameter values and comparisons are shown in Table 2.

Histopathological scores: In the histopathological examinations, it was determined thickness in interseptal areas, debris in bronchial, inflammatory cells infiltration and alveolar congestion in the section of groups (Fig. 1). In our histopathological examination, lung tissue's vascular characteristics were evaluated according to alveolar content and bronchiolar characteristics and scored. The scores were found to be lower in the control and SIL groups and significantly higher in the PAX group ($p<0.05$). These values were significantly lower in the PAX+SIL group than the PAX group ($p<0.05$). Histopathologic changes are seen in Fig. 1 and all scores are shown in Table 3.

Immunohistochemical results: In the immunohistochemical analysis, immune reactivity of Bax, iNOS, Nf-kB, IL-6 and MUC1 levels were higher in the PAX group than other groups ($p<0.05$). but, these reactivities were decreased in the PAX+SIL groups

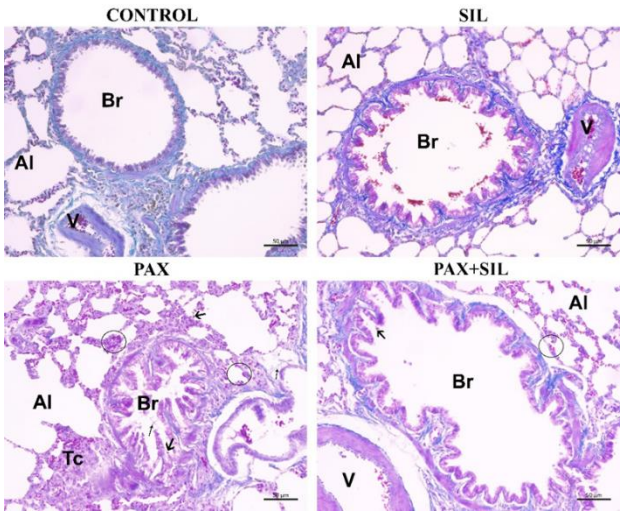

Fig. 1: Illustration of histologic lung section for all groups, Br; Bronchial, Al; Alveoli, Tc; thickness in interseptal areas, V: Arteriole, Long arrow; debris, arrow; inflammatory cells, circle; alveolar congestion, Crossman modified Triple staining, X200 Magnification.

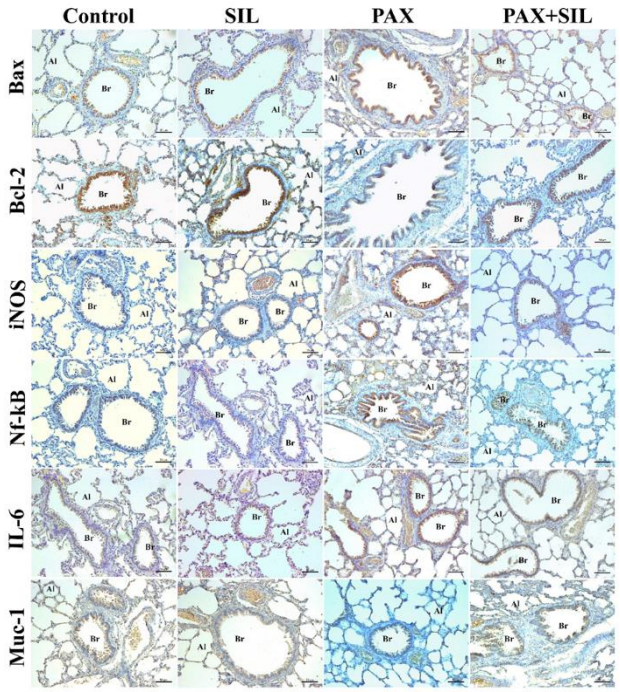

Fig. 2: Immunohistochemical illustration of lung sections staining with ani-Bax, anti-Bcl-2, anti-iNOS, anti- Nf-kB, anti-IL-6, and anti-Muc-1 antibodies, Br; Bronchiole, Al; Alveoli, Streptavidin–Biotin (LSAB) staining, X200 Magnification.

compared to PAX group. Also, there were no statistical differences between the SIL and control groups in regards of the Bax, iNOS, Nf-kB, and IL-6 immune reactivities ($p>0.05$). On the other hand, Bcl-2 immune reactivity was found lower in the PAX group, but higher in the PAX+SIL group ($p<0.05$). The immune reactivity of antibodies for all groups were presented in the Table 4. The immune reactions of tissue sections are seen Fig. 2.

Relative protein expression levels of Caspase-3, Bcl-2, IL-6, Nf-kB-p65 and P2X7R: In protein expression analysis, P2X7R, IL-6, Nf-kB-p65 and Caspase-3 expressions were found to be significantly higher in the PAX group, and significantly lower in control, SIL and PAX+SIL groups

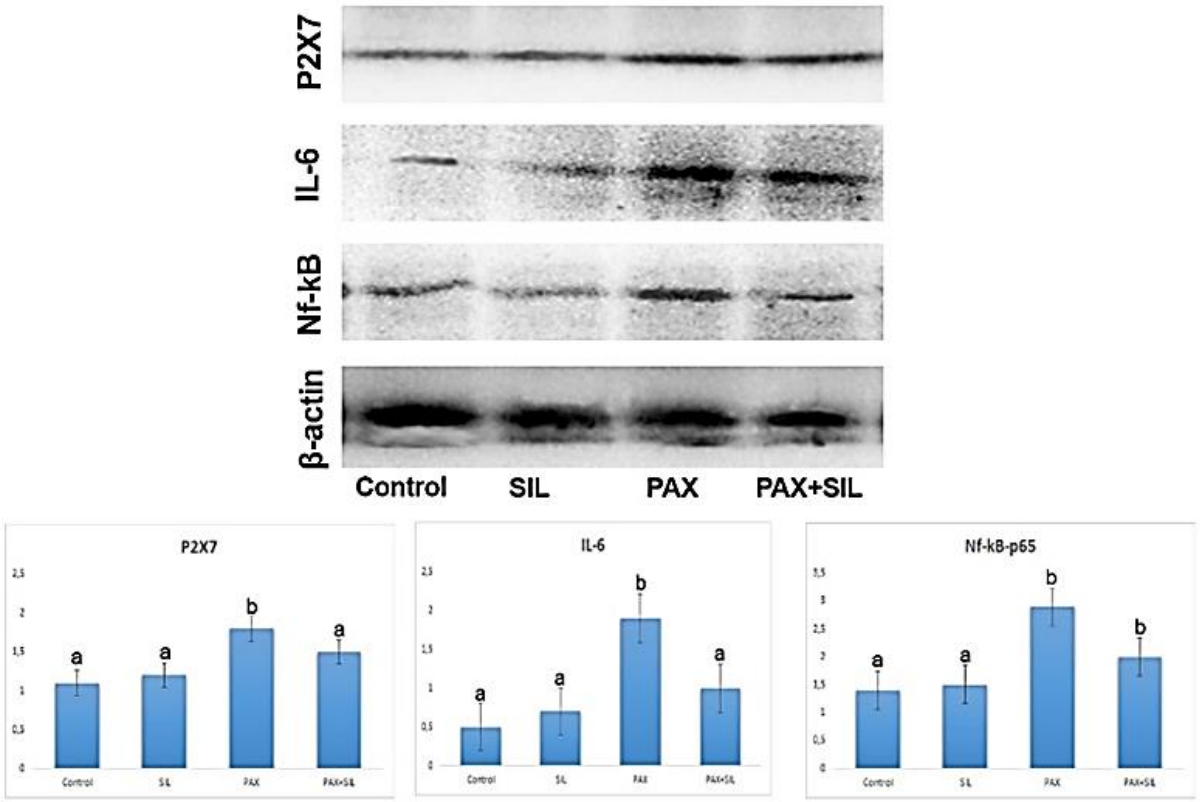

Fig. 3: Relative protein expression levels of P2X7R, IL-6 and Nf-kB-p65 for all groups using western blot technique, the values are expressed as mean ± standard deviation. The letters (a,b) indicate the statistical differences between groups in the same column.

Table 1: Lung histopathological evaluating scoring system

Score	Vascular features	Extravascular and alveolar involvement	Bronchiole features
0	Minimal	Minimal	None
1	Blood leaking into interstitium; mild RBC obstruction	Mild inflammatory exudate; areas of patchy edema with some disordered structure	Mild infiltration of inflammatory cells
2	Mild RBC and vascular obstruction; areas of mild and moderate congestion	Moderate inflammatory exudate; areas of moderate alveolar thickening (25–50% visualized lung)	Moderate infiltration of inflammatory cells; detachment of lining in some bronchioles

Table 2: Biochemical Malondialdehydes (MDA), glutathione (GSH), Superoxide dismutase (SOD), glutathione peroxidase (GPx), and Catalase (CAT) parameters for all groups.

Groups (n:6)	MDA (nmol/g tissue)	GSH (nmol/g tissue)	SOD (U/g protein)	GPx (U/g protein)	CAT (katal/g protein)
Control	37.91±2.57^{a}	1.50±0.08^{a}	21.82±1.45^{a}	28.95±1.58^{a}	38.10±1.62^{a}
SIL	37.58±1.90^{a}	1.59±0.08^{a}	23.87±1^{a}	30.01±0.91^{a}	39.04±1.83^{a}
PAX	61.95±2.50^{b}	1.04±0.07^{b}	15.68±0.93^{b}	18.84±0.90^{b}	22.70±1.47^{b}
PAX+SIL	52.20±2.83^{a}	1.28±0.07^{a}	19±0.77^{a}	23.88±1.29^{a}	29.44±1.15^{a}

The values are expressed as mean ± standard deviation. The letters (^{a,b,c}) indicate the statistical differences between groups in the same column.

Table 3: Histopathologic scores of lungs of all groups

Score Value (n:6)	Vascular features	Extravascular and alveolar involvement	Bronchiole features	Mean of scores
Control	0.17±0.41^{a}	0.33±0.52^{a}	0.17±0.41^{a}	0.22±0.44^{a}
SIL	0.33±0.52^{a}	0.14±0.38^{a}	0.14±0.38^{a}	0.20±0.29^{a}
PAX	2.5±0.55^{b}	2.33±0.52^{b}	2.17±0.75^{b}	2.33±0.61^{b}
PAX+SIL	1.85±0.69^{c}	1.57±0.53^{c}	1.85±0.9^{c}	1.76±0.71^{c}

Note: The values are expressed as mean ± standard deviation. The letters (^{a,b,c}) indicate the statistical differences between groups in the same column.

Table 4: Immunohistochemical evaluation of the Bax, Bcl-2, iNOS, Nf-kB, IL-6 and MUC1 reactivities for all groups.

Groups (n:6)	Bax	Bcl-2	iNOS	Nf-kB	IL-6	MUC1
Control	0.014±0.014^{a}	0.025±0.005^{a}	0.018±0.009^{a}	0.010±0.003^{a}	0.019±0.003^{a}	0.013±0.005^{a}
SIL	0.025±0.014^{a}	0.015±0.005^{a}	0.020±0.009^{a}	0.015±0.003^{a}	0.025±0.003^{a}	0.016±0.005^{a}
PAX	0.067±0.011^{b}	0.070±0.009^{c}	0.068±0.010^{c}	0.079±0.008^{b}	0.083±0.008^{b}	0.076±0.009^{b}
PAX+SIL	0.039±0.014^{c}	0.037±0.005^{c}	0.032±0.009^{a}	0.032±0.003^{c}	0.027±0.003^{a}	0.054±0.005^{c}

Note: The values are expressed as mean ± standard deviation. The letters (^{a,b,c}) indicate the statistical differences between groups in the same column.

($p<0.05$). Also, there was no significant differences in regards of P2X7, IL-6, Nf-kB-p65 and Caspase-3 immune reactivities between the SIL and Control groups ($p<0.05$). However, Nf-kB immune reactivity of PAX+SIL group was not significantly different from PAX group ($p<0.05$). Bcl-2 protein expression values were significantly higher in Control, SIL and PAX+SIL groups than the PAX group ($p<0.05$). The relative protein expression levels of the Caspase-3, Bcl-2, IL-6, Nf-kB-p65 and P2X7R were seen in the Fig. 3 and 4.

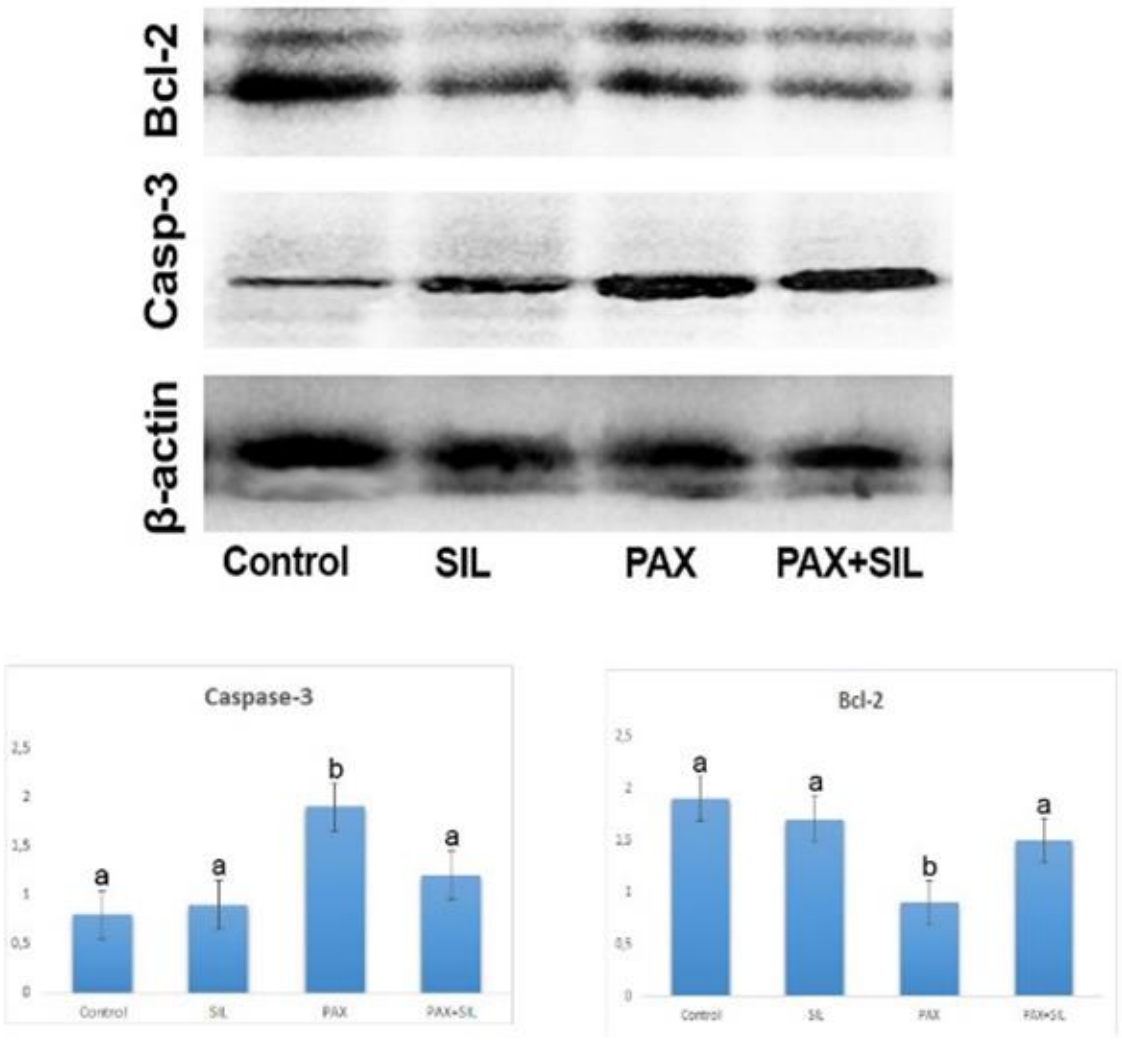

Fig. 4: Relative protein expression levels of Bcl-2 and Caspase-3 for all groups using western blot technique, the values are expressed as mean ± standard deviation. The letters (a,b) indicate the statistical differences between groups in the same column.

DISCUSSION

Paclitaxel is an agent that has caused significant advancements in chemotherapy in recent years (Barbuti and Chen 2015). Paclitaxel is one of the taxen group antineoplastic agents, and it prevents the transformation of microtubules to tubulins by binding to the β-tubulin group of microtubules during mitotic division. Thus, the destruction of spindles is prevented during mitotic division, and cell division is terminated (Giovinazzi *et al.*, 2016; Yasuhira *et al.*, 2016). However, as paclitaxel treatments might also damage healthy cells, the use of substances with antioxidant properties in combination with this agent is an issue that has been emphasized in recent years. Thus, this study aimed to increase the effectiveness of paclitaxel by combining silymarin with paclitaxel and eliminate oxidative stress in healthy cells.

In some studies, it was reported that silymarin stimulates tissue regeneration, facilitates DNA, RNA, and protein synthesis, eliminates reactive oxygen species, increases superoxide dismutase levels, and prevents peroxidation. At the same time, it was proven that silymarin protects the cell membrane thanks to its antioxidant properties in the studies (Milić *et al.*, 2013). In another study, cell lines treated with silymarin were shown to be more resistant to paclitaxel-induced cytotoxicity due to its high total antioxidant capacity. Additionally, antioxidants like superoxide dismutase, catalase and tiols (N-acetyl cysteine) also inhibit cytotoxicity (Hadzic *et al.*, 2010). In a study in which rats were given paclitaxel, various histopathological findings like widening in endoplasmic reticulums of type 2 alveolar cells and degeneration in mitochondria were reported. In a study by Liu *et al*. (2015) lung damage was produced with paclitaxel and with histopathological scoring made in lung tissue, disruption in alveolar structure, inflammation, hemorrhage, pulmonary interstitial edema, and thickening were seen. In another study, immune and nonimmune responses were seen like acute bilateral pneumonia, hypersensitivity reactions, and cytokine release from alveolar macrophages in patients treated with paclitaxel. In addition, pulmonary damage induced by paclitaxel is defined as subacute interstitial pneumonia, acute diffuse intersititial pneumonia, and noncardiogenic pulmonary edema. In the CLP sepsis model by Adiguzel *et al*. (2016) hemorrhage, edema, epithelial damage, and a significant decrease in neutrophil infiltration were found histopathologically in silymarin-applied rat lungs. In our study, with silymarin treatment a significant improvement was obtained in paclitaxel-induced lung damage and degeneration in vascular structure, increased

alveolar content, thickening in alveolar septa, and disruption in bronchiolar structure compared to the PAX group. This induced damage is in line with the literature above.

With the use of chemotherapeutic agents, reactive oxygen species (ROS) or free radicals are produced in cancer cells. That's why, serious side effects are observed in cancer treatment. Studies show that this oxidative damage might be decreased with natural compounds (Butt *et al.*, 2018). There is a delicate balance between free oxygen, antioxidants, and radicals in the body. Disruption of this balance in different directions is called oxidative stress. Oxidative stress might cause bio-molecular damage called lipid peroxidation. MDA is one of the products of lipid peroxidation which is an important marker of oxidative stress. The level of oxidative stress is regulated by both enzymatic and nonenzymatic antioxidant systems. SOD, GPx and CAT are enzymatic and GSH is a nonenzymatic antioxidant (Birben *et al.*, 2012; Kumar Arora and Kumar Singh, 2014). In our study, it was determined that while MDA levels significantly increased in the PAX group compared to the control group, GSH, SOD, GPx and CAT levels decreased. The results that paclitaxel use causes oxidative stress in lung tissue are parallel to the literature. Compared to the PAX group, MDA levels were lower, and GSH, SOD, GPx, and CAT levels were higher in the PAX+SIL group. Accordingly, silymarin decreases lipid peroxidation by antioxidant and free radical scavenging effects and by the way increases GSH, SOD, GPx and CAT concentrations. Thus, silymarin contributes cellular defence mechanism.

Apoptosis is a marker that results from excessive ROS levels and indicates that the inflammatory phase in the cell suddenly switches to the proliferative phase. During apoptosis, there are changes in the amount of Bax and Bcl-2 proteins that are members of the caspase family. Bax is proapoptotic, while Bcl-2 is an antiapoptotic protein (Cui *et al.*, 2018). In our study, dense Bax immunopositivity was detected in the PAX group, and thinner in Control, SIL, and PAX+SIL groups. When the sections were scored in terms of Bcl-2 immunopositivity, it was significantly thinner in the PAX group compared to the Control, while denser in control and silymarin treated SIL and PAX+SIL groups compared to the PAX group.

Transcription factor nuclear factor kappa B (NF-κB) is a dimeric transcription factor that is associated with the regulation of genes in pathological events like apoptosis and inflammation. Additionally, in a study, it was demonstrated that NF-κB inhibition with proteasome inhibitors increases apoptosis in lung adenocarcinoma cells (Milligan and Nopajaroonsri, 2001). The nuclear factor kappa-beta (Nf-κB) is a critical transcription factor that controls the expression of inflammation-related inducible nitric oxide (iNOS), adhesion molecules, and some other mediators. iNOS synthesis is known to be associated with Nf-κβ activation (Sordi *et al.*, 2015). In our study, Nf-κβ expression was shown to increase immunohistochemically in the PAX group. On the other hand, Nf-κβ expression was significantly lesser in the silymarin-treated group. It was also seen that with paclitaxel application iNOS expression increased and silymarin application suppressed iNOS activity. With all these results, silymarin application was shown to be effective against paclitaxel-induced rat lung damage, and decreased the damage by suppressing Nfκβ activity and iNOS synthesis.

Paclitaxel-induced lung tissues, and the use of Silymarin alleviated the P2X7R expression. Similar to the increase in P2X7R expression, tissue damage and cytokine generation increase with paclitaxel exposure, and Silymarin decreases tissue cytokine levels. It has been reported previously that in the inflammation process, P2X7R expression increases in immune response, and consequently, the generation of inflammation-mediated cytokine is stimulated (Kara and Ozkanlar, 2023). In addition, Silymarin reduces P2X7R expression and inhibits tissue damage caused by inflammation and the P2X7R inhibition also suppresses the production of chemokines (Xie *et al.*, 2013) . In other mechanism, NF-κB also induces the transcription of proinflammatory cytokines like TNF-α, and IL-6 that cause self-activation by providing a positive feedback mechanism because of its role in inflammation. IL-6 plays an important role in the immunity of the body and stress response and has both pro-inflammatory and anti-inflammatory effects (Heink *et al.*, 2017). Bcl-2 protein expression values were found to be significantly higher in Control, SIL, and PAX+SIL groups compared to the PAX group.

In conclusion, silymarin is therapeutically effective against lung damage resulting from paclitaxel treatment and it could help repair cellular damage and alleviate the P2X7R mediated inflammation and apoptotic cell death by in keeping oxidant-antioxidant balance and regulating of inflammatory mediator release. Future more detailed molecular studies are needed to elaborate metabolic pathways of these mechanisms.

Funding: This research received no external funding.

Credit author statement: We confirm that this work is original and has not been published elsewhere, nor is it currently under consideration for publication elsewhere.

Conflict of interest statement: The authors declare no conflict of interest.

Authors contributions: All authors contributed to this present work: NAC, HK, AK and EE participated in the design of the study. EE, HK, and AK performed the experiments. NAC, and EE acquired the data. AK analyzed the data. HK, and NAC drafted the manuscript. EE and HK revised the manuscript. All authors read and approved the final manuscript.

REFERENCES

Adiguzel SC, Pirat A, Turkoglu S, *et al.*, 2016. A rat model of acute respiratory distress silymarin's antiinflamatory and antioxidant effect. J Turk Soc Intens Care 14(1):18-27.

Aebi H, 1983. Catalase. In:Bergmeyer HU, ed. Methods in EnzymaticAnalysis. New York:Academic Press 276–286.18.

Amoateng P, Adjei S, Osei-Safo D, *et al.*, 2017. Analgesic effects of a hydro-ethanolic whole plant extract of Synedrella nodiflora (L.) Gaertn in paclitaxel-induced neuropathic pain in rats. BMC Res Notes 10(1):1-7.

Barbuti AM and Chen ZS, 2015. Paclitaxel through the ages of anticancer therapy:Exploring its role in chemoresistance and radiation therapy. Cancers 7(4):2360-2371.

Birben E, Sahiner UM, Sackesen C, *et al.*, 2012. Oxidative stress and antioxidant defense. WAO J 5(1):9-19.

Burnstock G, 2006. Pathophysiology and therapeutic potential of purinergic signaling. Pharmacol Rev 58(1):58-86.

Cheng KC, Asakawa A, Li YX, *et al.,* 2014. Silymarin induces insulin resistance through an increase of phosphatase and tensin homolog in Wistar rats. PLoS One 9(1):e84550.

Cui J, Wang G, Kandhare AD, *et al.,* 2018. Neuroprotective effect of naringin, a flavone glycoside in quinolinic acid-induced neurotoxicity:possible role of PPAR-γ, Bax/Bcl-2, and caspase-3. Food Chem Toxicol 121:95-108.

Çelik H, Kandemir FM, Caglayan C, *et al.,* 2020. Neuroprotective effect of rutin against colistin-induced oxidative stress, inflammation and apoptosis in rat brain associated with the CREB/BDNF expressions. Mol Biol Rep 47(3):2023-2034.

Butt SL, Saleemi MK, Khan MZ, *et al.,* 2018. Cadmium toxicity in female Japanese quail (Coturnix japonica) and its diminution with silymarin. Pak Vet J 38:249-255.

Erbaş E, Gedikli S, Taghizadehghalehjoughi A, et al., 2023. Investigation of the curative effects of Hypericum perforatum (St. John's Wort) and Rosa spinosissima (Black rosehip) on rats in an indomethacin-induced gastric peptic ulcer model. GSC Biol Pharmaceut Sci 22(3):243-252.

Giovinazzi S, Bellapu D, Morozov VM, *et al.,* 2013. Targeting mitotic exit with hyperthermia or APC/C inhibition to increase paclitaxel efficacy, Cell Cycle 12(16):2598-2607.

Hadzic T, Aykin-Burns N, Zhu Y, *et al.,* 2010. Paclitaxel combined with inhibitors of glucose and hydroperoxide metabolism enhances breast cancer cell killing via H2O2-mediated oxidative stress. Free Radic Biol Med 48(8):1024-1033.

Heink S, Yogev N, Garbers C, *et al.,* 2017. Trans-presentation of IL-6 by dendritic cells is required for the priming of pathogenic TH 17 cells. Nat Immunol 18(1):74-85.

Gür C, Özkanlar S, Gedikli S, *et al.,* 2022. The effects of quercetin administration on heart tissue and serum parameters in the rats with experimental obesity. Eurasian Mol Biochem Sci 1(1):16-21.

Kara A and Ozkanlar S, 2023. Blockade of P2X7 receptor-mediated purinergic signaling with A438079 protects against LPS-induced liver injury in rats. J Biochem Mol Toxicol 37(10):e23443.

Kumar Arora M and Kumar Singh U, 2014. Oxidative stress:meeting multiple targets in pathogenesis of diabetic nephropathy. Curr Drug Targets 15(5):531-538.

Le B, Khorsi-Cauet H, Bach V, *et al.,* 2012. Mast cells mediate Pseudomonas aeruginosa lipopolysaccharide-induced lung inflammation in rat. Eur J Clin Microbiol Infect Dis 31(8):1983-1990.

Liu W, Zhong Z, Cao, L, *et al.,* 2015. Paclitaxel-induced lung injury and its amelioration by parecoxib sodium. Sci Rep 5(1):1-9.

Matkovics B, 1988. Determination of enzyme activity in lipid peroxidation and glutathione pathways. Laboratoriumi Diagnosztika, 15, 248-250.

Milić N, Milošević N, Suvajdžić L, *et al.,* 2013. New therapeutic potentials of milk thistle (Silybum marianum). Nat Prod Commun 8(12):1801-10. PMID:24555302.

Milligan SA and Nopajaroonsri C, 2001. Inhibition of NF-kappa B with proteasome inhibitors enhances apoptosis in human lung adenocarcinoma cells in vitro. Anticancer Res 21(1A):39-44.

Passmore MR, Byrne L, Obonyo NG, *et al.,* 2018. Inflammation and lung injury in an ovine model of fluid resuscitated endotoxemic shock. Respir Res 19(1), 1-10.

Aydemir Celep N, Gedikli S, Parlak SN, *et al.,* 2023. Experimental hypothyroidism increases oxidative stress and apoptosis in ovary of rats. Eurasian Mol Biochem Sci 2(2):21-29.

Sedlak J and Lindsay RH, 1968. Estimation of total, protein-bound, and nonprotein sulfhydryl groups in tissue with Ellman's reagent. Anal Biochem 25:192-205.

Sordi R, Chiazza F, Johnson FL, *et al.*, 2015. Inhibition of IκB kinase attenuates the organ iniury and dysfunction associated with hemorrhagic shock. Mol Med 21(1):563-575.

Sun Y, Oberley LW and Li Y, 1988. A simple method for clinical assay of superoxide dismutase. Clin Chem 34(3):497-500.

Taleb A, Ahmad KA, Ihsan AU, *et al.,* 2018. Antioxidant effects and mechanism of silymarin in oxidative stress induced cardiovascular diseases. Biomed Pharmacother 102:689-698.

Yardım A, Kucukler S, Özdemir S, *et al.,* 2021. Silymarin alleviates docetaxel-induced central and peripheral neurotoxicity by reducing oxidative stress, inflammation and apoptosis in rats. Gene 15;769:145239.

Xie Y, Williams CD, Mc Gill MR, *et al.,* 2013. Purinergic receptor antagonist A438079 protects against acetaminophen-induced liver injury by inhibiting p450 isoenzymes, not by inflammasome activation. Toxicol Sci 131(1):325-335.

Yasuhira S, Shibazaki M, Nishiya M, *et al.*, 2016. Paclitaxel-induced aberrant mitosis and mitotic slippage efficiently lead to proliferative death irrespective of canonical apoptosis and p53, Cell Cycle 15(23):3268-3277.